Available online at www.sciencedirect.com
ScienceDirect
Bioorganic & Medicinal Chemistry Letters 18 (2008) 2346–2350
Bioorganic & Medicinal Chemistry Letters

Pharmacophore identification of Raf-1 kinase inhibitors

Tian Zhu,[a] Yu Jiao,[b] Ya-Dong Chen,[b] Xuan Wang,[a] Hui-Fang Li,[b] Lu-Yong Zhang[a] and Tao Lu[b,*]

[a]*National Drug Screening Laboratory, China Pharmaceutical University, 1 Shennong Road, Nanjing 210038, PR China*
[b]*Department of Organic Chemistry, China Pharmaceutical University, 24 Tongjiaxiang, Nanjing 210009, PR China*

Received 24 September 2007; revised 9 February 2008; accepted 28 February 2008
Available online 4 March 2008

Abstract—A three-dimensional pharmacophore model was developed based on 25 currently available Raf-1 kinase inhibitors. The best pharmacophore hypothesis (Hypo1), consisting of four chemical features (one hydrogen-bond acceptor, one hydrogen-bond donor, and two hydrophobic groups), has a correlation coefficient of 0.972. The results of our study provide a valuable tool in designing new leads with desired biological activity by virtual screening.

The Ras-MAP kinase pathway has a central role in regulating tumor cell growth and survival, differentiation and angiogenesis and has been targeted for therapeutic intervention in the past.[1,2] The Raf-1 (also termed as c-Raf) kinase is required for Ras signal transduction and is the first enzyme in a MAP kinase cascade consisting of the three protein kinases Raf-1, MEK, and ERK. Disruption of this cascade at various points inhibits Ras signal transduction and transformation in many experimental systems.[3–5] Raf-1 also contributes to tumorigenicity by negatively regulating apoptosis through direct interaction with bcl-2 family members.[6–8] Thus, selective inhibitors of the Raf-1 kinase may prove to be effective broad-spectrum antitumor agents and have the potential to enhance existing cancer chemotherapies.

At the end of 2005, Bayer and Onyx launched a new anti-cancer drug named Sorafenib (tosylate salt of BAY 43-9006). It mainly targets Raf-1 kinase and possesses excellent activity and extremely low side effects. During the past several years, several Raf-1 kinase inhibitors have been reported.[9–16] The increasing knowledge of the Raf-1 kinase structure, activity and regulation, together with the generation of new data, is giving momentum to the development of ligand-based design. In a ligand-based design, identification of a pharmacophore is one of the most important steps. In this paper, we identified pharmacophore model of the Raf-1 kinase inhibitors for the first time and explained it using a homology model of the Raf-1 kinase.

The study was performed using the Catalyst software package (version 4.11, Accelrys Inc., San Diego, CA) on a SGI Origin 3800 workstation. Chemical-feature-based pharmacophore hypotheses can be generated automatically using the HypoGen algorithm within Catalyst, provided that structure–activity relationship data of a well-balanced set of compounds are available.

Twenty-five compounds (Nos. **1**–**25** in Fig. 1) forming the training set were used to generate HypoGen hypotheses by considering structural diversity and wide coverage of activity in terms of IC_{50} ranging from 1.4 nM to 50 μM (Table 1). All structures in the training set were built and minimized to the closest local minimum based on a modified CHARMM force field within the Confirm module. Catalyst generated a representative family of conformational models for each compound using a Monte–Carlo-like algorithm together with Poling.[17] This method uses a poling function that prevents conformations of molecules from being too close together and allows the exploration of the conformational space of molecules within a user-defined energy threshold. Diverse conformational models for each compound were generated using an energy range of 20 kcal/mol of the calculated potential energy minimum. Specify 250 as the maximum number of conformers of each molecule to ensure maximum coverage of the conformational space.

Keywords: Raf-1 kinase; Pharmacophore; Homology modeling; Docking.
* Corresponding author. Tel.: +86 25 86185180; fax: +86 25 86185179; e-mail: lutao@cpu.edu.cn

0960-894X/$ - see front matter © 2008 Elsevier Ltd. All rights reserved.
doi:10.1016/j.bmcl.2008.02.068

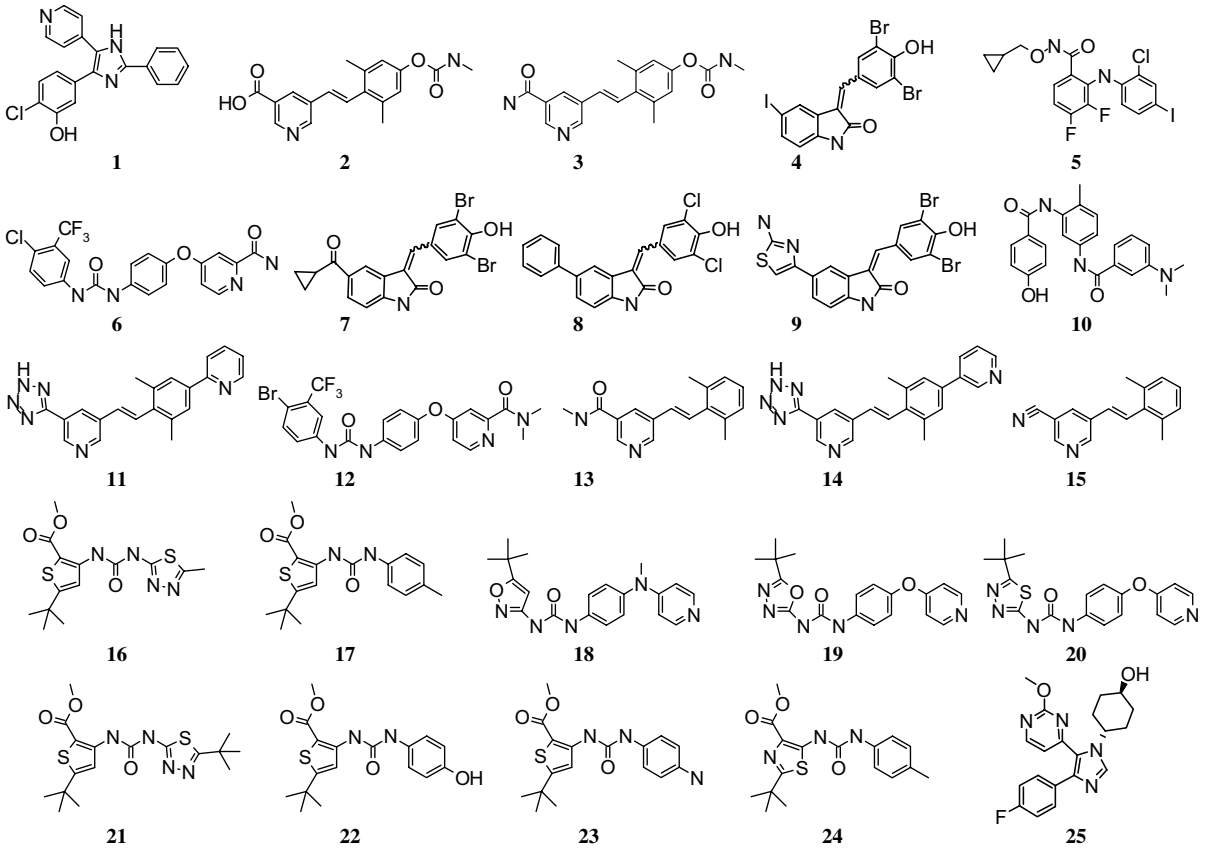

Figure 1. 2D chemical structures of the 25 molecules forming the training set used to obtain HypoGen pharmacophore hypotheses.

Table 1. Experimental biological data and estimated IC_{50} values of the training set molecules based on the pharmacophore model Hypo1

Compound	Experimental IC_{50} (nM)	Estimated IC_{50} (nM)	Error	Reference
1	1.4	2.7	+1.9	16
2	6	5.8	−1.0	13
3	7	3.8	+1.8	13
4	9	28	+3.1	10
5	12	9.7	−1.2	15
6	13	16	+1.2	12
7	25	110	+4.5	10
8	32	150	+4.7	10
9	46	120	+2.6	10
10	70	120	+1.7	13
11	100	280	+2.8	16
12	170	160	−1.0	12
13	250	200	−1.3	13
14	630	290	−2.1	13
15	1000	250	−3.9	13
16	1200	1100	−1.1	11
17	1700	1400	−1.2	11
18	3500	2400	−1.5	12
19	6300	8200	+1.3	12
20	8600	6100	−1.4	12
21	11,000	4700	−2.3	11
22	15,000	8800	−1.7	11
23	18,000	11,000	−1.6	11
24	25,000	7300	−3.4	11
25	50,000	31,000	−1.6	14

Taking into account the chemical nature of the compounds considered in this work, the following four criteria were selected to form the pharmacophore hypothesis generation process: hydrogen-bond acceptor (HBA), hydrogen-bond donor (HBD), hydrophobic group (Hp), and ring aromatic (Ar). The uncertain factor for each compound represents the ratio range of uncertainty in the activity value based on the expected statistical straggling (the square root of the variance) of biological data collection. Here, we use default uncertainty value 3. Pharmacophores were then computed using HypoGen module implemented in Catalyst software package and the top 10 scoring hypotheses were exported (Table 2). In order to determine whether our quantitative model is statistically significant, able to identify active structures and forecast their activity accurately, two validation procedures were followed namely: cost analysis and test-set prediction.

Catalyst produced 10 hypotheses (Hypo1–Hypo10). Hypo1, which consisted of four features: one hydrogen-bond acceptor (HBA), one hydrogen-bond donor (HBD), and two hydrophobic (Hp) groups were found to be the best pharmacophore hypothesis in this study (Fig. 2). This is characterized by the highest cost difference, lower error cost, lowest root mean square (rms) divergence, and best correlation coefficient (Table 2). The null cost of the 10 top-scored hypotheses was equal to 185.371, the fixed cost value was 103.043, and the configuration cost was 15.828. As the total cost of

Table 2. Information of statistical significance and predictive power presented in cost values for top 10 hypotheses[a]

Hypothesis	Features	Total cost	Δcost	Rms	Correlation (*r*)
1	ADHH	112.582	72.789	0.705	0.972
2	ADHH	116.639	64.305	0.974	0.940
3	AHHR	124.415	58.934	1.295	0.887
4	DHHR	124.800	57.532	1.371	0.870
5	ADHH	126.472	57.469	1.400	0.866
6	ADHH	126.516	56.934	1.358	0.875
7	AAHH	126.665	56.746	1.400	0.865
8	ADHH	128.353	56.723	1.390	0.870
9	AAHH	129.450	56.403	1.482	0.847
10	ADHH	129.550	55.469	1.401	0.868

[a] Abbreviations used for features: A, hydrogen-bond acceptor; D, hydrogen-bond donor; H, hydrophobic group; R, aromatic ring.

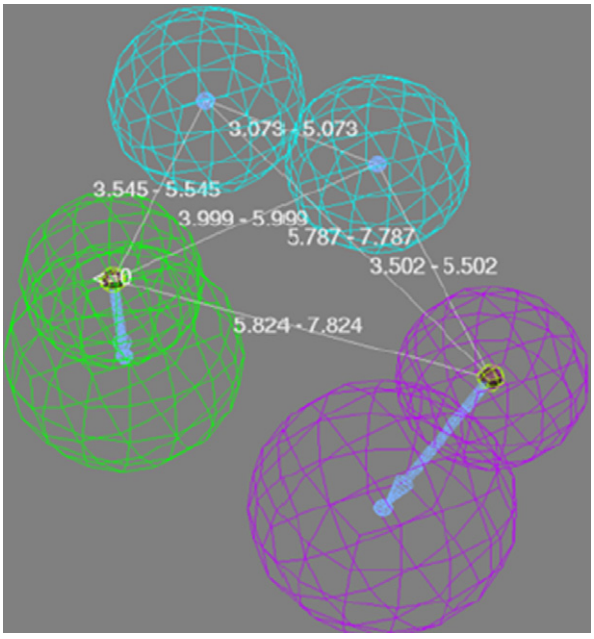

Figure 2. Top-scoring HypoGen pharmacophoreol. Features are color-coded as follows: hydrogen-bond acceptor green; hydrophobic, blue; hydrogen-bond donor, violet.

Hypo1 was equal to 112.582, the large difference between null and total hypothesis cost, (Δcost) 72.789, coupled with a high correlation coefficient, (*r*) 0.972 (Fig. 3), and a reasonable root mean square (rms) deviation 0.705 ensures that a true correlation will very likely be estimated by the model. The total cost represents the combined error of estimation as calculated by the ratios between experimental and estimated activities, the deviation of the feature weights from the ideal weight, and the complexity of the hypothetical space; the null cost pertains to a hypothesis with no features which assumes there is no relationship between structure and activity for the entire training set. Remarkably, the most active compounds (compounds **2** and **6**) can be well mapped onto the Hypo1 model, (Fig. 4), indicating that the Hypo1 model provides reasonable pharmacophoric characteristics of the Raf-1 inhibitors for the components of their activities. Then 20 compounds of

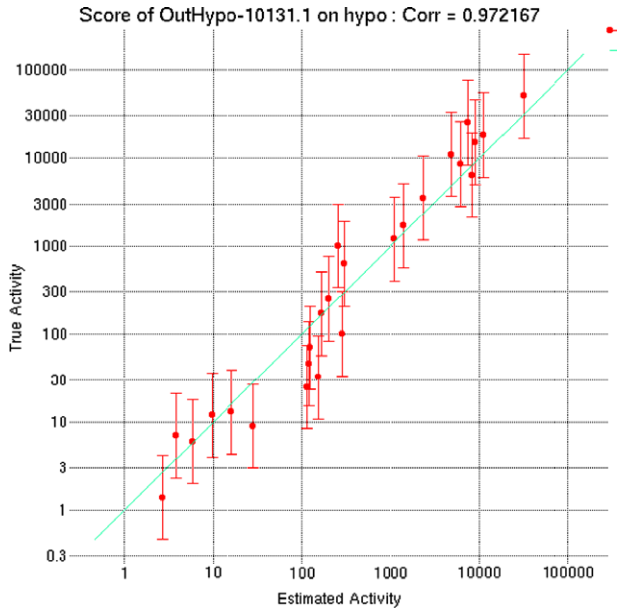

Figure 3. The regression of actual versus predicted, activities by the Hypo1 hypothesis for the training set inhibitors onto a linear relationship.

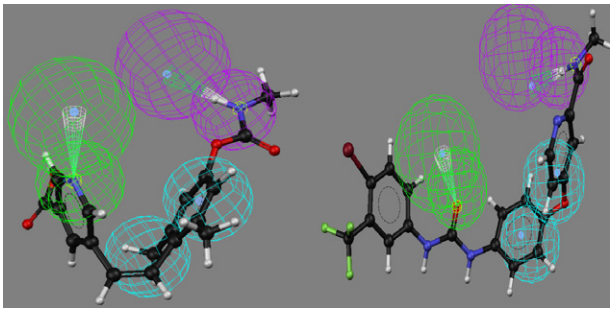

Figure 4. Depicts compound **2** (left) and compound **6** (right) mapping of Hypo1.

the test set (Nos. **26**–**45** in Fig. 5) were mapped onto the best pharmacophore hypothesis Hypo1. A correlation coefficient of 0.916 generated using the test set compounds shows a good correlation between the actual and estimated activities. As we can see from Table 3, all the error values were found to be less than 10, which means a not-more-than one order difference between estimated and actual activity.

A homology model of the Raf-1 kinase was built to analyze the ligand–protein interaction. The tertiary structure of Raf-1, for which a crystal structure is not available, was constructed by homology modeling using the crystal structure of the kinase domain of human wild type B-Raf and V599E B-Raf. In homology modeling, 3D structure of homologous protein is used as a template to construct unknown structure. The alignment of human Raf-1 (Entrez Protein: P04049),[18] wild type B-Raf and V599E B-Raf domain amino acid sequences was refined in Swiss-PDBViewer.[19,20] The 3D structure modeling and refinements were carried out using InsightII. The model was finally minimized with CVFF force fields and the final structure was further checked

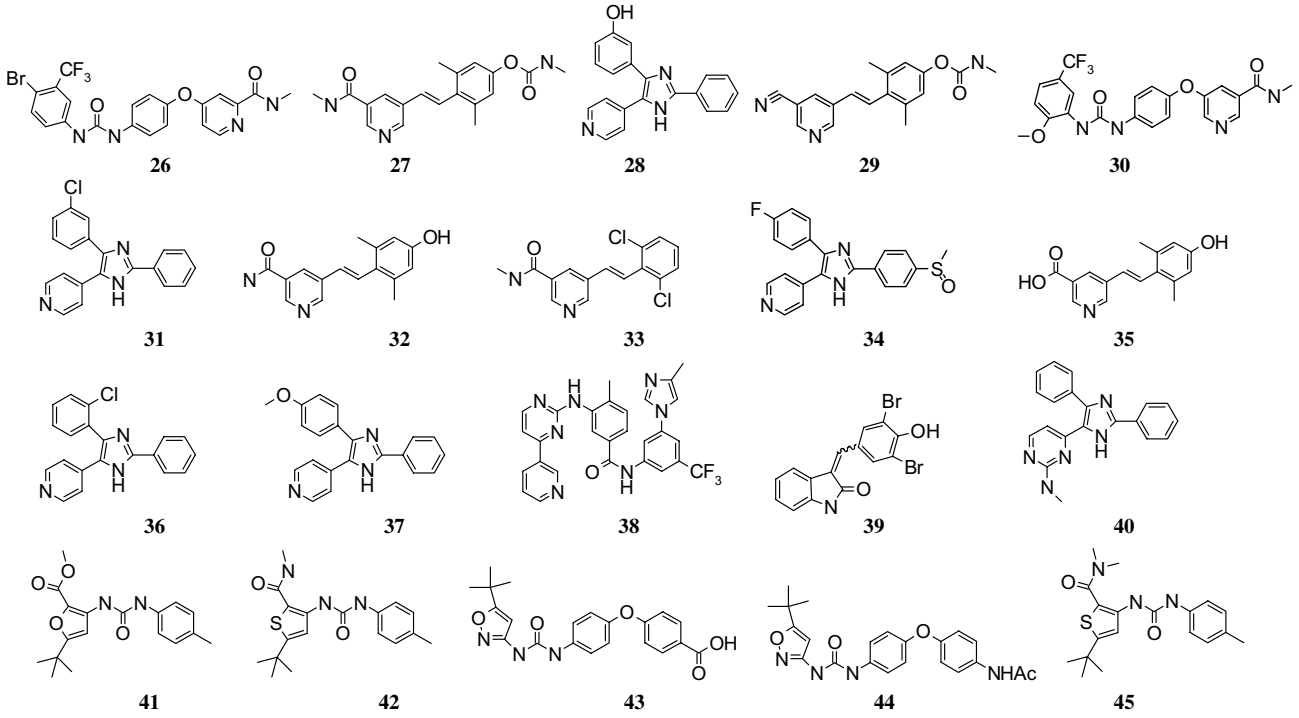

Figure 5. 2D chemical structures of the 20 molecules forming the testing set.

Table 3. Experimental biological data and estimated IC_{50} values of the test set molecules based on the pharmacophore model Hypo1

Compound	Experimental IC_{50} (nM)	Estimated IC_{50} (nM)	Error	Reference
26	6	14	+2.3	12
27	10	13	+1.3	13
28	23	37	+1.6	9
29	40	72	+1.8	13
30	61	370	+6.0	12
31	90	410	+4.6	9
32	158	140	−1.1	13
33	251	250	−1.0	13
34	330	420	+1.3	9
35	398	590	+1.5	13
36	610	390	−1.6	9
37	950	770	−1.2	9
38	1100	190	−5.8	16
39	1300	210	−6.2	16
40	2100	1700	−1.2	9
41	3000	5300	+1.8	12
42	4900	4800	−1.0	11
43	6300	4400	−1.4	11
45	15,000	11,000	−1.4	11

through PROFILE-3D program resulting in that all residues are scored positive, which means that these residues are reasonable.[21]

The protein and ligands were saved in a mol2 format with the aid of Sybyl 6.9. Docking studies were performed with AutoDock 3.0.5 using a Lamarckian genetic algorithm.[22] The standard docking procedure was used for a rigid protein and a flexible ligand whose torsion angels were identified (for 100 independent runs per ligand).

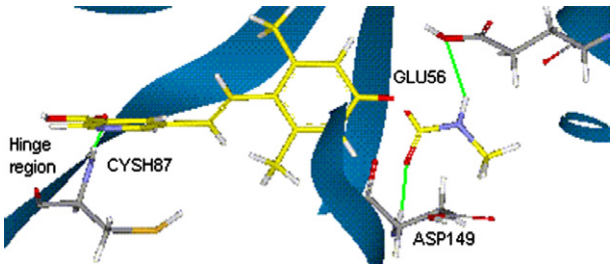

Figure 6. Stereoviews of the docked conformation of compound **2** in the active site of Raf-1.

Illustrated in Figure 6 is a docking model of compound **2** in complex with the Raf-1 kinase. The inhibitor's pyridyl ring binds to the kinase at the hinge region with its nitrogen atom forming an H-bond interaction with the backbone NH of Cys87. The 4-hydroxy-2,6-dimethylphenyl moiety is positioned deep into the ATP-binding pocket and is surrounded by mostly hydrophobic residues. It also forms an H-bond interaction with the side chain of Glu56 through the carbamate NH. The additional H-bond interaction is formed between the inhibitor's carbonyl and the backbone NH of Asp149. Illustrated in Figure 7 is a docking model of compound **6** in complex with the Raf-1 kinase. The 4-pyridyl ring bearing amide group is located in the ATP-binding pocket by forming a hydrogen-bond with Cys87 involving amide NH group. Three hydrogen-bonds are formed between urea group and the Raf-1 kinase. Two of them are formed with Glu56; the additional is formed with the backbone NH of Asp149. The trifluoromethyl phenyl ring is located in the hydrophobic pocket formed between C and E helices and forming a hydrogen-bond with Thr63. We hypothesize that besides the necessary

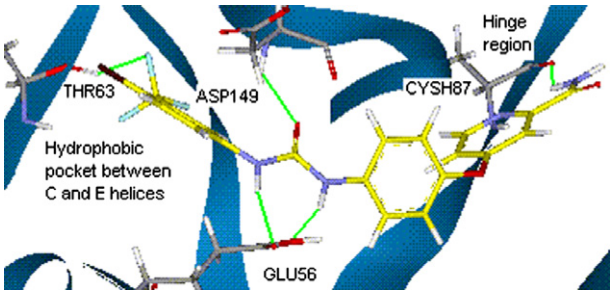

Figure 7. Stereoviews of the docked conformation of compound **6** in the active site of Raf-1.

pharmacophore indicated in Hypo1, additional substituents that combine both electronegative and lipophilic properties are preferred in the hydrophobic pocket formed between C and E helices, which may increase the stability and potency.

In summary, a three-dimensional pharmacophore model was developed based on 25 inhibitors of the Raf-1 kinase by a ligand-based computational approach. This pharmacophore hypothesis consists of one hydrogen-bond acceptor, one hydrogen-bond donor, and two hydrophobic groups, and has a correlation coefficient of 0.972. Besides, this hypothesis is further validated by using an external test set of 20 compounds. The most active compounds fit very well with this top-scoring hypothesis. Furthermore, we built a homology model of the Raf-1 kinase to analyze the interaction between ligands and the Raf-1 kinase. Accordingly, our pharmacophore model should be helpful in identifying novel lead compounds with improved inhibitory activity through 3D database searches and providing a valuable tool in designing new inhibitors of the Raf-1 kinase.

Supplementary data

Supplementary data associated with this article can be found, in the online version, at doi:10.1016/j.bmcl.2008.02.068.

References and notes

1. Herrera, R.; Sebolt-Leopold, J. S. *Trends Mol. Med.* **2002**, *8*, S27.
2. Chang, F.; Steelman, L. S.; Lee, J. T.; Shelton, J. G.; Navolanic, P. M.; Blalock, W. L.; Franklin, R. A.; McCubrey, J. A. *Leukemia* **2003**, *17*, 1263.
3. Kolch, W.; Heidecker, G.; Lloyd, P.; Rapp, U. R. *Nature* **1991**, *349*, 426.
4. Monia, B. P.; Johnston, J. F.; Geiger, T.; Muller, M.; Fabbro, D. *Nat. Med.* **1996**, *2*, 668.
5. Davies, H.; Bignell, G. R.; Cox, C.; Stephens, P.; Edkins, S.; Clegg, S.; Teague, J.; Woffendin, H.; Garnett, M. J.; Bottomley, W.; Davis, N.; Dicks, E.; Ewing, R.; Floyd, Y.; Gray, K.; Hall, S.; Hawes, R.; Hughes, J.; Kosmidou, V.; Menzies, A.; Mould, C.; Parker, A.; Stevens, C.; Watt, S.; Hooper, S.; Wilson, R.; Jayatilake, H.; Gusterson, B. A.; Cooper, C.; Shipley, J.; Hargrave, D.; Pritchard-Jones, K.; Maitland, N.; Chenevix-Trench, G.; Riggins, G. J.; Bigner, D. D.; Palmieri, G.; Cossu, A.; Flanagan, A.; Nicholson, A.; Ho, J. W.; Leung, S. Y.; Yuen, S. T.; Weber, B. L.; Seigler, H. F.; Darrow, T. L.; Paterson, H.; Marais, R.; Marshall, C. J.; Wooster, R.; Stratton, M. R.; Futreal, P. A. *Nature* **2002**, *417*, 949.
6. Gajewski, T. F.; Thompson, C. B. *Cell* **1996**, *87*, 589.
7. Wang, H.; Rapp, U. R.; Reed, J. C. *Cell* **1996**, *87*, 629.
8. Wang, H.-G.; Takayama, S.; Rapp, U. R.; Reed, J. C. *Proc. Natl. Acad. Sci. U.S.A.* **1996**, *93*, 7063.
9. Nigel, J. L.; John, W. B.; Christopher, F. C.; David, A. C.; Brian, E. L.; Kevin, T. N.; Steven, M. P.; Harold, G. S.; Garry, R. S.; Andrew, T.; Joseph, P. V.; Sandor, L. V.; Lily, A.; Kim, D.; Amy, J. F.; Daniel, S. F.; Betsy, F.; William, A. H.; Coral, F. H.; Scott, J. H.; Matthew, K.; Jiunn, L.; Sylvie, L.; Edward, A. O'N.; Chad, J. O.; Margaret, P.; Janey, P.; Anna, R.; Yousif, S.; Denise, M. V.; Stephen, J. O'K. *J. Med. Chem.* **1999**, *42*, 2180.
10. Karen, L.; Michael, C.; Ronda, D.; Stephen, V. F.; Philip, A. H.; Robert, N. H.; David, K. J.; Bradley, M.; Robert, W. M.; Michael, R. P.; Randy, D. R.; James, M. V.; Edgar, R. W. *Bioorg. Med. Chem. Lett.* **2000**, *10*, 223.
11. Roger, A. S.; James, B.; Cheri, L. B.; Mark, A. B.; Yolanda, V. C.; Robert, D.; Jeffrey, S. J.; Michael, E. K.; Nancy, K.; Jill, K.; Wendy, L.; Timothy, B. L.; John, L.; Vivienne, M.; Daniel, H. R.; Stephen, S.; Tracy, W.; Hanno, W. *Bioorg. Med. Chem. Lett.* **2001**, *11*, 2775.
12. Ram, T.; Pankaj, D.; Shaikh, A. R.; Rahul, B.; Javed, I. *Bioorg. Med. Chem.* **2004**, *12*, 6415.
13. Octerloney, M.; Karen, L.; Ronda, D.; Edgar, W.; Vicente, S.; Patrick, M.; Felix, D.; Robert, H. *Bioorg. Med. Chem. Lett.* **2006**, *16*, 5378.
14. David, C. U.; Ruth, R. O.; Charles, J. K.; Jerry, L. A.; John, C. L.; Edward, F. W.; Donald, C. C.; Steven, B.; Heath, C. T.; Douglas, W. P. H.; Don, E. G. *J. Pharmacol. Exp. Ther.* **2000**, *293*, 281.
15. Boris, W. K.; Rudolf, G.; Ulf, R. R. *BMC Cancer* **2004**, *4*, 24.
16. Roger, A. S.; Jacques, D.; Lila, A.; Scott, M. W. *Curr. Top. Med. Chem.* **2006**, *6*, 1071.
17. Smellie, A.; Kahn, S. D.; Teig, S. *J. Chem. Inf. Comput. Sci.* **1995**, *35*, 285.
18. Bonner, T. I.; Oppermann, H.; Seeburg, P.; Kerby, S. B.; Gunnell, M. A.; Young, A. C.; Rapp, U. R. *Nucleic Acids Res.* **1986**, *14*, 1009.
19. PDB deposition number: 1UWH.
20. PDB deposition number: 1UWJ.
21. Sali, A.; Blundell, T. L. *J. Mol. Biol.* **1993**, *234*, 779.
22. Dauber-Osguthorpe, P.; Roberts, V. A.; Osguthorpe, D. J.; Wolff, J.; Genest, M.; Hagler, A. T. *Proteins* **1988**, *4*, 31.